KSR INSTITUTE FOR ENGINEERING AND TECHNOLOGY

KSRIET
Where future begins...

THE DEPARTMENT MAGAZINE

Department of Mechanical Engineering

MECH ZINE

VOLUME 3 ISSUE 2

The Gear of Tomorrow

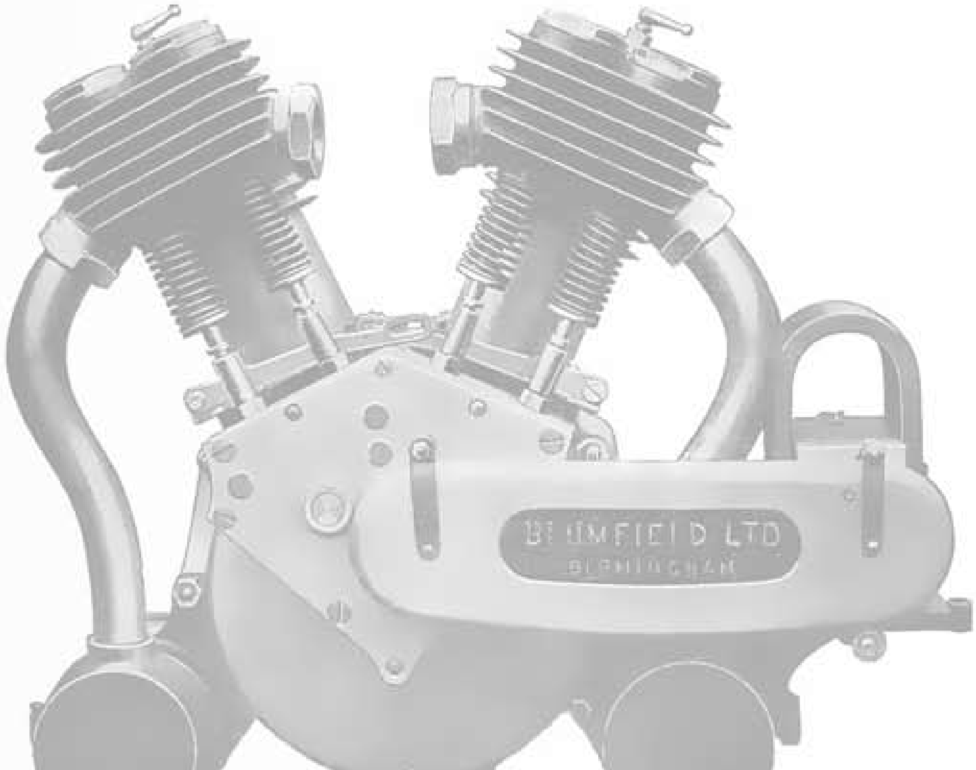

If its broken,
take it apart
and fix it.

ACADEMIC YEAR 2016 - 2017

KSR INSTITUTE FOR ENGINEERING AND TECHNOLOGY

Vision

To become a globally recognized Institution in Engineering Education, Research and Entrepreneurship.

Mission

IM1	Accomplish quality education through improved teaching learning process
IM2	Enrich technical skills with state of the art laboratories and facilities
IM3	Enhance research and entrepreneurship activities to meet the industrial and societal needs

DEPARTMENT OF MECHANICAL ENGINEERING

Vision

To produce globally recognized Mechanical Engineers and Entrepreneurs to meet the industrial challenges with ethical values.

Mission

DM1	Impart quality education in Mechanical Engineering through enhanced teaching learning process.
DM2	Provide platform to apply and analyze the engineering concepts with state of the art laboratories.
DM3	Augment the technical knowledge among students and faculty members through research activities to meet industrial and societal needs.

Program Educational Objectives (PEOs)

PEOs	Keywords	Description
PEO1	**Core Competency**	Graduates will adopt technological changes in core and allied areas of Mechanical Engineering.
PEO2	**Professionalism**	Graduates will have leadership quality with soft skills to excel in their professional career.
PEO3	**Higher Studies and Entrepreneurship**	Graduates will evoke interest in higher education and develop entrepreneurial attitude for ever changing industrial and societal environment.

MECHZINE

MECH ZINE
VOLUME 3 ISSUE 2

DRAWING FROM OUR STUDENTS ON ASSOCIATION FUNCTION

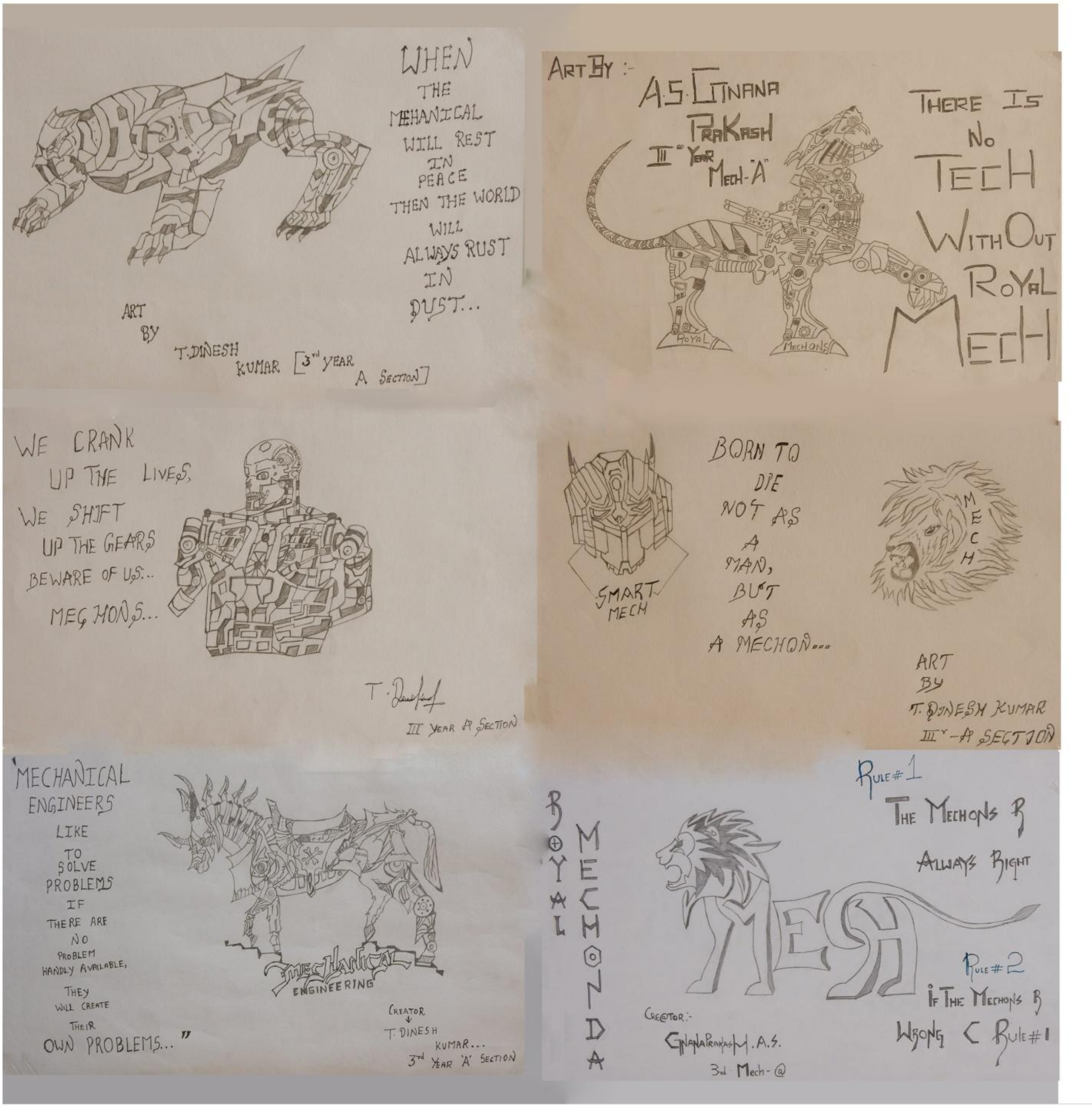

The design and analysis of a high-speed circular arc gear pump journal bearing

S.K. Pugazhendi, II Year, Department of Mechanical Engineering, KSRIET

A series of problems arise when a gear pump operates at high speed, including instability of the rotor, deformation of the chamber, and wear of the journal bearing. Among all failure modes, journal bearing wear is the most serious. The wear of journal bearings of a circular arc gear pump that operates at high speed is thus presented in this article. A journal bearing that offsets the unbalanced radial force is designed by analysis of the fluid and determination of eccentricity of the gear shaft. Experiments show that the wear of the new journal bearing is effectively reduced.

The development trend of the gear pump is that the pump is operated at high speed. However, a series of problems arise at high speed, resulting in research on the design of the tooth profile, research on processing methods, fluid analysis, and analysis of performance. Some problems that arise when a gear pump operates at high speed have been solved theoretically. However, the wear of a gear pump is difficult to analyze theoretically. Moreover, the wear of a gear pump results in instability of the rotor, damage to the pump body, and an increase in the temperature of the hydraulic oil. Mucchi E et al. established a mathematical model that can be used to optimize the running-in process and to investigate the effect of wear of the pump casing. Koç E and Hooke C J studied the wear of loaded floating.

mrek H and Düzcükoğlu H reduce noises and vibrations caused by wear in spur gears by tooth modification. Thiagarajan D improve lubrication performance and reduces wear in external gear pump by tooth profile design. Kwon S-M optimized the shape of a gear using a genetic algorithm to reduce contact stress and gear wear. Wang X investigated the wear of a gear pump using omega theory and validated their results with experimental results. Frith RH and Scott W verified the wear model of a gear pump with experimental results. Koç E studied the lubrication of bush-type bearings operating at high pressure, revealing that lubrication between end faces of the gear and bush-type bearings depends on the surface irregularities and non-flatness. Cha M studied the effect of the tilt of journal bearings and showed the relationship between the thickness and pressure of the oil film. Yang H discussed the effects of installation errors, hydraulic oil contamination, and manufacturing precision on the wear of journal bearings. Jolly P studied the characteristics of a hydrostatic journal bearing for an aerospace turbo pump. The angle of the oil injection hole and the shape and size of the internal groove were determined by numerical analysis. At the same time, the flow rate of the sliding bearing was measured. Static and dynamic experiments verified the correctness of the theory. Naïmi S et al. focused on the load capacity of journal bearings using a circumferential central feeding groove and discussed the effect of the pressure of the oil film and eccentricity of journal bearings. Dhawan R and Verma Sstudied journal bearing lubrication employing a finite element method for hydrostatic. The bearing behavior of a hydrostatic bearing under a heavy load was analyzed from the viewpoint of tribology, and a method of improving the bearing capacity of the interaction bearing was discussed. Costa L through set the oil groove on hydrostatic bearing to improve lubrication. The above studies revealed that the most common form of failure is wear between the inner wall of a journal bearing and the rotor.

In all wear of a gear pump, the journal bearings are obvious. This wear is caused by an unbalanced radial force. However, the research cited above rarely mentioned how to solve the effect of unbalanced radial force acting on a gear pump. The present paper thus designs journal bearings that offset part of the radial force. The design is verified experimentally.

This section uses a circular arc gear pump as a basic model. The radial force is determined by the design of the teeth and obtained by establishing a mathematical model of high- and low-pressure zones. Journal bearings that offset the unbalanced radial force are then designed.

The circular gear pump comprises a driving gear, driven gear, journal bearings, pump body, front end cover, rear end cover, and oil seal, as shown in Figure 1. A three-dimensional model of a journal bearing is shown in fig

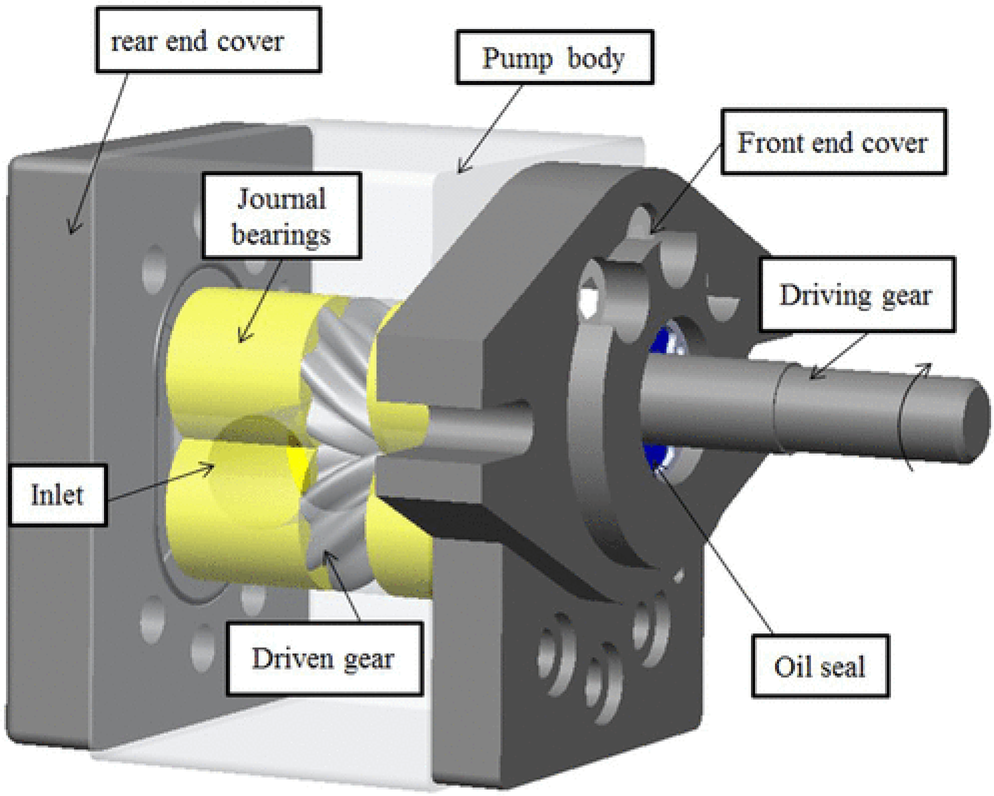

Figure 1. Structure of a circular arc gear pump.

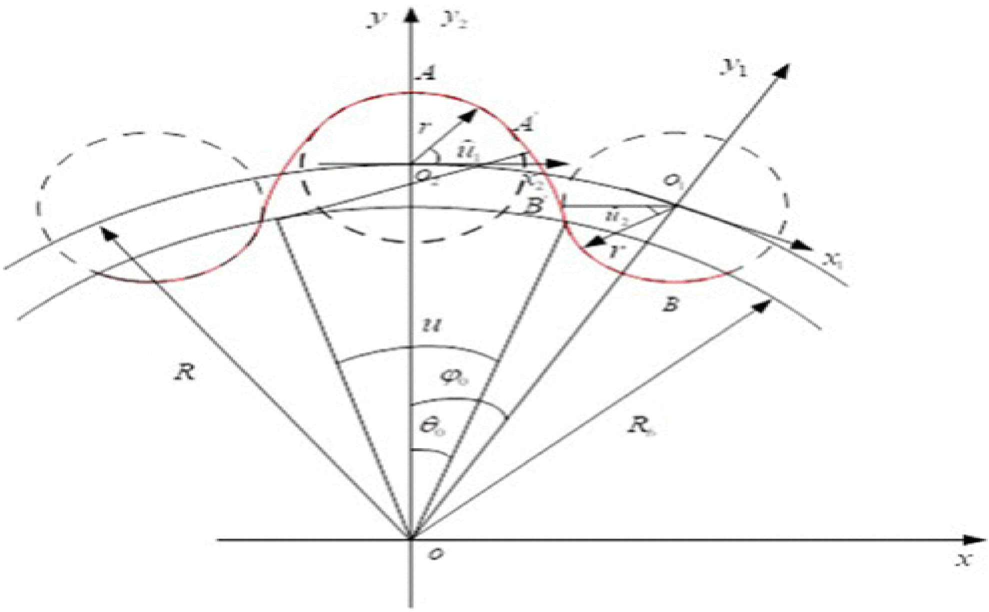

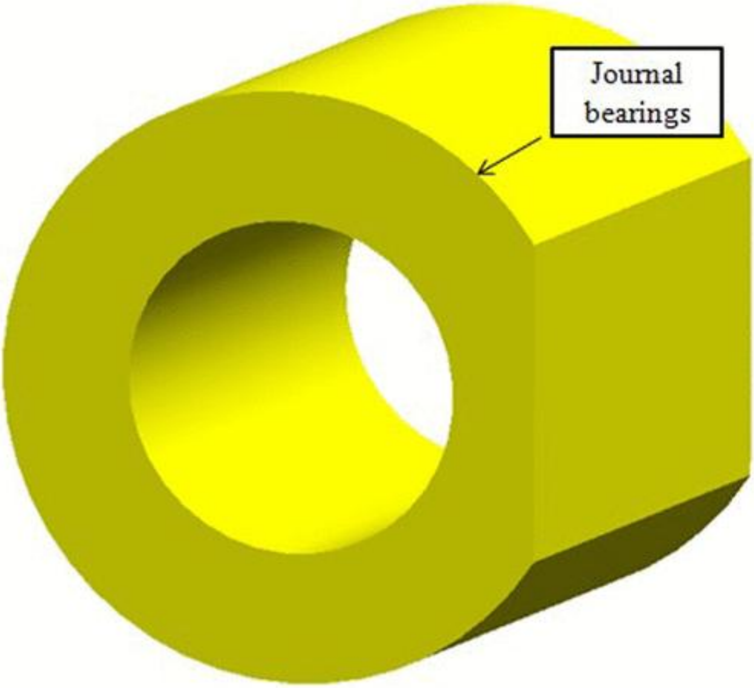

Figure 2. Three-dimensional model of journal bearing.

The circular arc tooth is formed by circular arc AA', involute $A'B'$, and circular arc BB'.

Analysis of vehicle static steering torque based on tire–road contact patch sliding model and variable transmission ratio

M. Prasanakumar, II Year, Department of Mechanical Engineering, KSRIET

Static steering torque at parking is an important factor for steering portability of vehicle. At present, the most commonly used estimation method is empirical formula calculation, which, however, cannot explain the phenomenon that the steering torque increases rapidly when steering angle becomes very large (over 300°). This article proposes an estimation method of static steering torque on the basis of a mathematic model of tire-patch sliding torque, taking into account the changeable torque transmission ratio from steered wheel to steering wheel. Three components of static steering torque are modeled and analyzed, including the tire-patch sliding torque, gravity aligning torque, and internal friction torque of the steering system. In order to investigate the static steering torque at steering wheel, the transmission ratio of steering torque is obtained on the basis of rack-suspension mathematical analysis. An example of static steering torque estimation is conducted with the proposed method and is compared with experimental results. The comparison shows that the estimation results given by the proposed method are in better accordance with experimental results than other approaches.

Vehicle steering performance can be described in two general ways, that is, steering stability and portability. Steering stability indicates vehicle stability during steering, while the steering portability refers to the ability of steering at parking or low speed when steering torque is at its highest in steering maneuvers. For steering stability, many tire models including the magic formula model have been used to investigate tire force distribution, especially the lateral force during driving. However, few tire models or estimation methods for investigation of static steering torque have been proposed to study the steering portability. At present, static steering torque is mostly calculated by empirical formula, assuming that the tire–road contact patch is similar to a circle. However, the tire–road contact patch is much closer to a rectangle for radial tire, and the assumption of a circular tire–road contact patch usually gives a large computation error when used to calculate the static steering torque of radial tire.

Static steering torque is a key component for assist characteristic design of power steering system, which determines the drivers' steering portability on parking. However, the static steering torque model presented by empirical formula, which is adopted to design static power steering characteristic, has low accuracy and often results in bad feeling in static steering maneuvers. Automatic parking systems, such as parking assistance system (PAS), the advanced parking assistance system (APAS), and autonomous valet parking (AVP), are all low-velocity system, and most of the researches focus on the path design and control of parking, but the realization of automatic parking needs precision control of steering motor, and an accurate static steering torque model is therefore necessary for parking motor control. The parking system of intelligent vehicle is similar to automatic parking system. Without supervision and participation of the driver, the parking motor control needs more precise static steering model. The power steering system and automatic parking system mentioned above are basic systems in modern automobile; the importance of static steering torque for these systems makes the study of static steering a focus in the field of steering studies. In addition, the tire steering torque during the process beginning from vehicle's start to the time it reaches a low velocity (about 10 km/h) has been a difficult problem, and precision static steering model contributes to the investigation of this issue.

Static steering torque is usually described by the feedback of steering wheel torque, which includes the internal friction torque of steering system, the gravity aligning torque generated by vertical force, and the tire-patch sliding torque (tire-patch sliding torque is the sliding torque acting on the tire–road contact patch). The tire-patch sliding torque is usually regarded as static steering torque for simplicity because it accounts by far for the largest proportion of it. Static steering torque increases linearly in traditional calculation, but the actual steering torque increases rapidly when steering angle becomes very large (over 300°). The reason is that the traditional method does not take into consideration the change of torque transmission ratio from steered wheel to steering wheel. Because of the large steering angle in static steering maneuver, the torque transmission ratio experiences a big change, which cannot be ignored.

Aiming at studying the static steering torque, tire-patch sliding torque on the basis of rectangular contact patch assumption is analyzed in this article. The gravity aligning torque is analyzed, and the internal friction torque of steering system is also measured. The transmission ratio from steered wheel to steering wheel is estimated in order to obtain a more precise value of the torque. In section "Static steering torque model," the static steering torque is investigated, including the tire-patch sliding torque and gravity aligning torque. The transmission ratio is investigated on the basis of mathematic and kinematic analysis of steering system in section "Transmission ratio of torque." The estimation method and results of static steering torque are given in section "Static steering torque estimation and test results," including the comparison of estimation results and test results. The conclusion is given in the final section.

High mechanical advantage design of six-bar Stephenson mechanism for servo mechanical presses

L. Vignesh, III Year, Department of Mechanical Engineering, KSRIET

This article proposed a two-phase design scheme of Stephenson six-bar working mechanisms for servo mechanical presses with high mechanical advantage. In the qualitative design phase, first, a Stephenson six-bar mechanism with a slide was derived from Stephenson six-bar kinematic chains. Second, based on the instant center analysis method, the relationship between mechanical advantage and some special instant centers was founded, and accordingly a primary mechanism configuration with high mechanical advantage was designed qualitatively. Then, a parameterized prototype model was established, and the influences of design parameters toward slide kinematical characteristics were analyzed. In the quantitative design phase, a multi-objective optimization model, aiming at high mechanical advantage and dwelling characteristics, was built, and a case design was done to find optimal dimensions. Finally, simulations based on the software ADAMS were conducted to compare the transmission characteristics of the optimized working mechanism with that of slide-crank mechanism and symmetrical toggle mechanism, and an experimental press was made to validate the design scheme. The simulation and experiment results show that, compared with general working mechanisms, the Stephenson six-bar working mechanism has higher mechanical advantage and better dwelling characteristics, reducing capacities and costs of servo motors effectively.

Servo mechanical presses are novel metal forming equipments utilizing servo drive technology. They can offer the flexibility of hydraulic presses and productivity of mechanical presses, being propitious to improve the forming limit, product accuracy, and working environment.

The most common working mechanism for traditional mechanical presses is the slide-crank mechanism (SCM) with a heavy flywheel mounted on the high-speed shaft. The flywheel, accumulating the mechanical energy during empty stroke and releasing the stored energy during forming, can reduce the capacity and restrain the speed variation of the induction motor (IM). The flywheel, however, is disadvantageous for servo mechanical presses, which pursue low inertia because of the increasing demands on the flexibility of slide motion. Therefore, for most servo mechanical presses, flywheels have to be removed and the forming forces are supplied totally by servo motors (usually, permanent magnet synchronous motors (PMSMs)). Hence, when common SCMs with low mechnical advantage are adopted as working mechanisms of servo presses, the capacities of PMSMs would have to been increased greatly, which raising manufacturing costs and hindering development and popularity of servo mechanical presses, especially the large-tonnage ones.

Generally, mechanical transmission system of servo mechanical presses includes driving elements, reducing mechanisms, and working mechanisms. In order to develop mechanical servo presses with large tonnage and low costs, several approaches are studied to develop new driving technologies or transmission mechanisms.

One of them is to develop hybrid driving technology, in which a large IM with constant speed and a small PMSM with variable speed were integrated together. The output motions from the IM and PMSM were synthesized by a 2 degree-of-freedom hybrid drive mechanism. Du and Guo, Meng, Li and Zhang, Guo and Ouyang conducted the studies on a 7R-type seven-bar linkage. He Tang and Guo, and Soong conducted the studies on a 5R2P-type seven-bar linkage. Li and Tso and Liang conducted the studies on a nine-bar linkage. Tokuz and Jones and Wang conducted the studies on a differential gearbox.

Another approach is to develop novel transmission mechanisms to cut down the capacities of PMSMs. Guo and colleagues proposed a parallel kinematic mechanism (PKM)-type transmission mechanism based on a parallel mechanism and a dual screw transmission mechanism. Sun and Suzuki and Hata adopted double reducing mechanisms to increase reduction ratio.

In the former case, the hybrid driving technology combines advantages of the inexpensive IM and flexible PMSM; however, the uncontrollability of the IM makes it difficult for the slide to stop or turn around in the approaching stroke, which are demanded by some sheet metal forming technologies, such as blending, coining, deep drawing, hot stamping, and so on, introduced by Osakada Moreover, due to the dynamic interaction of the two motors of different types, they have to counteract in power to obtain some required slide motion trajectories.

In the latter case, the adoption of parallel mechanisms will not cut down the total required capacities of PMSMs, but increasing the complexity for synchronization control. And too high reduction ratio will decrease the production efficiency of mechanical presses to an unacceptable degree, because the rated speed of large capacity servo motor is usually just a few hundred rotations per minute.

This article focuses on the development of Stephenson six-bar mechanisms (SSMs) with high mechanical advantage to cut down the capacities of servo motors. First, an instant center analysis method was presented to design qualitatively the primary mechanism configuration with high mechanical advantage, and then, a multi-objective optimization method was employed to synthesize the dimensions of the mechanism. Instant center analysis method has been successfully applied to the design of automobile rear suspension systems[2] and optical adjusting mechanisms, proven to be a visual, qualitative analysis technology. While, the multi-objective optimization design method is an analytic, quantitative technology. Hwang employed a multi-objective optimization method to synthesize the drag-link of mechanical press for precision drawing. In that case, the objective functions include the maximum normal force on the guide, mean mechanical advantage, variance of the drawing speed, and so on. In order to optimize the balancing design of the drag-link drive with adding disk counterweights, Chiou used a multi-objective optimization method to minimize the fluctuations of the shaking force and shaking moment. Smaili and Diabapplied an ant-gradient algorithm to solve the multi-objective dimensional synthesis problem of planar four-bar mechanisms, by considering transmission angle and mechanical advantage constraint into the objective function.

The purpose of this study is to propose a two-phase design scheme, qualitative and quantitative, to obtain a Stephenson six-bar working mechanism with high mechanical advantage for 1 degree-of-freedom servo mechanical presses, reducing the required PMSM capacity and improving the controllability, without decreasing the production efficiency. In the qualitative design phase, the relationship between mechanical advantage and instant centers is built and used to find the mechanism configuration with high mechanical advantage. While in the quantitative design phase, a multi-objective optimization model, with mechanical advantage, low-speed characteristics, and slow-moving uniformity of the slide being considered into objective functions, is constructed and solved. And some simulation and experiment studies were done to validate the design results.

The six-bar linkage of four binary bars and two ternary bars has two valid isomers, Watt's chain and Stephenson's chain. The six bars and seven joints of the Stephenson six-bar linkage compose one four-bar loop and one five-bar loop. It has two ternary links that are separated by a binary link, as shown in Figure 1. Once link 1 is chosen as the frame, link 2 as the input crank, and the revolute pair between links 6 and 1 is evolved into a sliding pair, a Stephenson-type six-bar mechanism with a slide can be derived, as shown in Figure 2. The continuous rotation of input crank 2 can be converted into a reciprocation of slide 6, which can be used as a working mechanism for servo mechanical presses. It should be noted that, being different from the conventional toggle mechanism, the connecting rod 3 of the SSM is a ternary link, which will bring about different transmission characteristics.

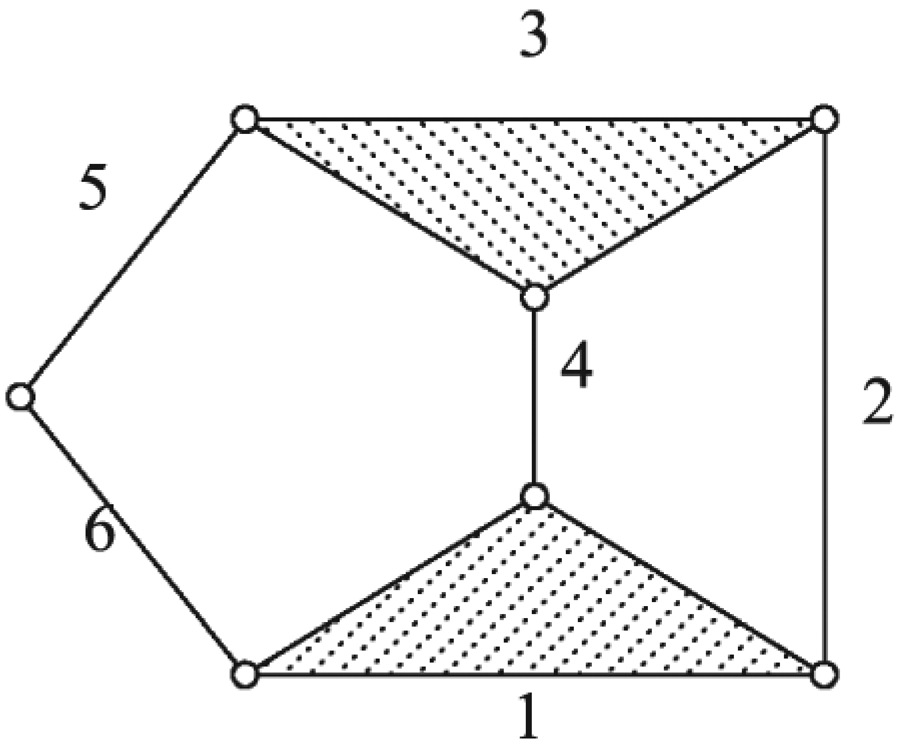

Figure 1. Stephenson six-bar kinematic chain.

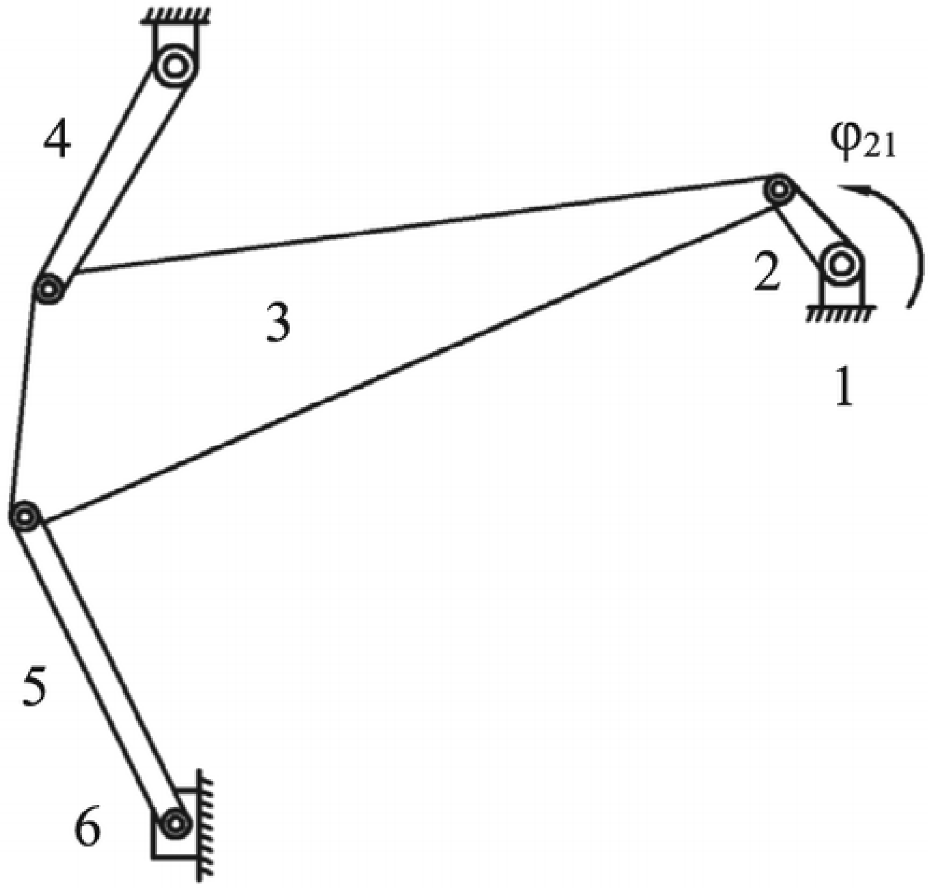

Figure 2 Type six-bar mechanism

Mechanical characterization of actomyosin complex by molecular mechanics simulations

G. Surya, IV Year, Department of Mechanical Engineering, KSRIET

Muscle contraction occurs when the actin and myosin filaments are driven past each other. There is a longrunning debate concerning the mechanism of the interaction between myosin and actin and the most widely accepted model proposed is the “lever-arm hypothesis” (1), which assumes that, after the myosin is firmly attached to the actin filaments, conformational changes in the molecule cause the swinging of the neck against the head called “power stroke” and generate mechanical force (1-3). The in vitro motility assay, combined with X-ray crystallography and molecular biology techniques, provided new experimental findings leading to new concepts in the molecular basis of muscle contraction, which consists of a cyclical interaction between myosin and actin driven by the concomitant hydrolysis of adenosine triphosphate (ATP) (4). According to Hodge and Cope (5), 17 different classes of myosin molecules are identified: two-headed conventional myosins are grouped into class II, classic single-headed unconventional myosins into class I, and the rest is divided into classes numbered in order of their discovery (6).

Actin filaments are helical polymers made up of G-actin monomers spaced by 5.5 nm, arranged in six left-handed turns repeating every 36 nm (8). G-actin is a highly conserved eukaryotic protein and, crystallographic studies show that it consists of two similar domains, each containing a 5-stranded β-sheet and associated α-helices. Each domain of the actin molecule can be further subdivided into two subdomains, termed 1, 2, 3, and 4 (Fig. 1b), which are stabilized by bonds to an adenine nucleotide and an Mg2+ cation. In the filament model, subdomains 3 and 4 form the core of the filament, while subdomains 1 and 2 project toward the periphery. Most of the amino acids that are involved in the interaction with myosin are located in subdomain

Knowledge of the mechanical properties of actin and myosin is fundamental to understand better the molecular mechanics of sliding force generation. For this reason, in recent years, different experimental studies have been carried out in order to measure mechanical parameters such as stiffness and elastic modulus. Experiments performed by Suda et al (9) with the rabbit skeletal muscle myosin II head under compression, estimated the value of the elastic modulus from the forcedistance profile. Later a similar experiment was performed to test directly the elastic properties of genetically engineered myosin II from Dictyostelium (10). Both experiments led to comparable results in terms of elastic modulus (0.3 GPa and 0.7 GPa, respectively). Concerning the elastic constants of the actin filaments, Blange et al (11) obtained an elastic modulus of 0.044 GPa, and Liu et al (12) found a stretching stiffness of 34.5 ± 3.5 pN/ nm using microfabricated cantilevers. The stiffness of 1 μmlong actin filaments with and without tropomyosin determined by

Kojima et al (13) using microneedles is 65.3 ± 6.3 and 43.7 ± 4.6 pN/nm, respectively. Individual behavior of molecular motors was successfully studied at the single molecule level. Several techniques have been developed to measure forces of protein bonds in the range from subpiconewtons to one nanonewton. Nishizaka et al used optical tweezers under a fluorescence phase-contrast microscope to measure the force required to unbind a rigor bond formed between an actin filament and a single myosin molecule (S1 and S2) in the absence of ATP. The average unbinding force was 9.2 ± 4.4 pN, only 2-5 times larger than the sliding force (16), but an order of magnitude smaller than interaction forces between antigen-antibody complex (17) or P-selectin-ligand complex

Model building

The atomic structures of myosin II and actin were taken from the RCSB Protein Data Bank. Mechanical properties of myosin were studied using the atomic coordinates set by Fisher et al (19) in 1MMD. pdb file, which is a 3-D structure of the myosin head from Dictyostelium discoideum complexed with beryllium fluoride (BeFx) and magnesium-ADP (MgADP), obtained through X-ray technique, with 2.0 Å resolution. The Dictyostelium myosin II was genetically truncated after residue 761, eliminating the lever arm and the associated light chains. Since the distance between β-phosphate of ADP and BeFx resemble the distance between the β- and γ-phosphate of the ATP, it had been suggested that this complex is an analog of the myosin-ATP state (19). Although the binding of ADP·BeFx decreases the affinity of myosin for actin, the crystal structure obtained with these ligands is remarkably similar to that observed in the 3-D model of chicken skeletal muscle myosin S1 in which no nucleotide was present

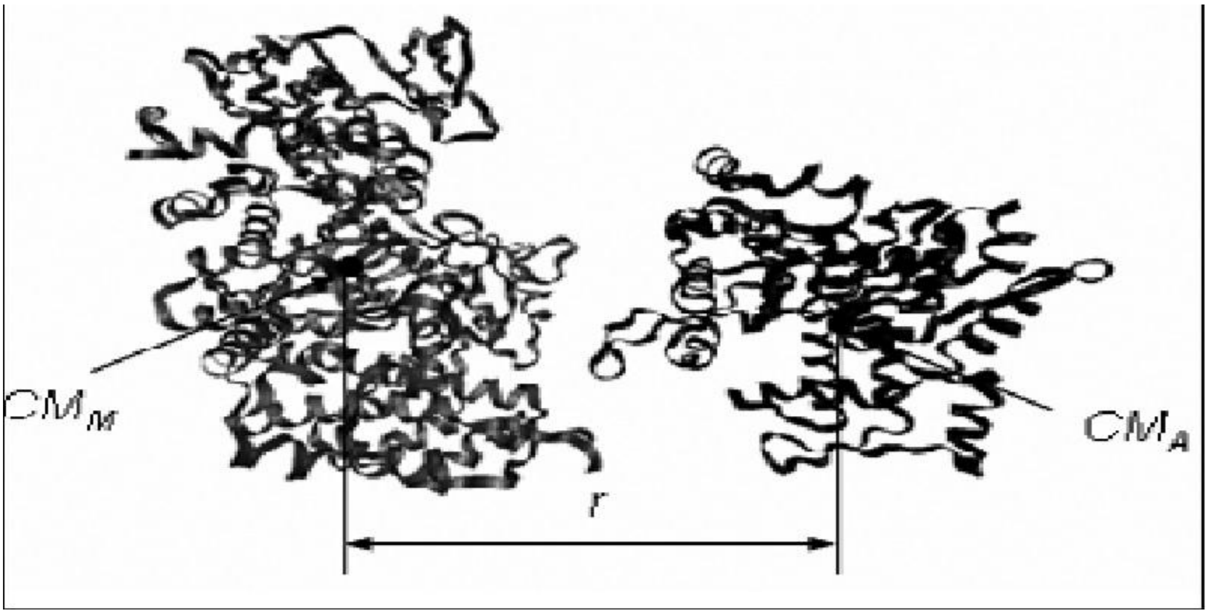

Multi-objective optimization of flexure hinge mechanism considering thermal–mechanical coupling deformation and natural frequency

R. Vignesh, IV Year, Department of Mechanical Engineering, KSRIET

Flexure hinge mechanism is generally used to obtain terminal nano-positioning using flexure hinges.1 With the outstanding features of no friction losses, no backlash, no need for lubrication, ease of fabrication, and virtually no assembly,2 flexure hinge mechanism can best achieve ultra-positioning in one dimension. Therefore, it could be employed to achieve a variety of application requirements in a variety of fields including microelectronic manufacture, nano-scale science and technology, optical and photon engineering, and so on.3–5

1School of Mechanical and Electrical Engineering, Henan University of Technology, Zhengzhou, P.R. China 2School of Mechanics Engineering, Zhongyuan University of Technology, Zhengzhou, P.R. China 3State Key Laboratory for Manufacturing Systems Engineering, Xi'an Jiaotong University, Xi'an, P.R. China 4Harbin Institute of Technology Shenzhen Graduate School, Shenzhen, P.R. China

Corresponding author: Lufan Zhang, School of Mechanical and Electrical Engineering, Henan University of Technology, Zhengzhou, Henan 450000, P.R. China. Email: zzzhanglufan@163.com

In order to obtain high performance, flexure hinge mechanism is usually studied by building accuracy prediction model and so on. The accuracy error is verified by simulation and experiment. Kang and Gweon presented an analytic model of cartwheel flexure. The model error was \10%, and its prediction accuracy relative to finite element method (FEM) simulations is satisfactory.6 Long et al. focused on error analysis of stiffness in right-angle flexure hinged double-parallel four-bar mechanism. It is concluded that the length ratio is between 6 and 25, and the thickness is .6 in the design.7 Li et al. proposed a power-function-shaped flexure hinge. The closed-form compliance equations of the flexure hinge were derived to design the powerfunction-shaped flexure hinges and could achieve higher motion accuracy than the commonly used circular flexure hinge and V-shaped flexure hinge.8 Qin et al. established the linear and angular compliance models for a class of statically indeterminate symmetric (SIS) flexure structures. An error model was established and incorporated into the analytical compliance models to function as an error compensator. Utilizing the error compensator, the modeling accuracy of the compliance models could be improved, which was validated by the experimental results on a flexure-based mechanism.9 Lobontiu formulated a matrix method for modeling the quasi-static response of planar serial flexure hinge mechanisms. The method was illustrated by a displacement–amplification mechanism with right circularly corner-filleted flexure hinges.10 Chen et al. obtained generalized equations for both the bending and the tension stress concentration factors for two generalized models, the conic model and the ellipticarc-fillet model. The empirical equations were tractable and easy to be employed in the design and optimization of flexure-based mechanisms. The case studies of the bridge-type displacement amplifiers demonstrated the effectiveness of the generalized equations for predicting the maximum stresses in flexure-based mechanisms.11 Meng et al. investigated the existing stiffness equations for corner-filleted flexure hinges. A total of three empirical stiffness equations for corner-filleted flexure hinges were formulated based on finite element analysis (FEA) results for the purpose of overcoming these investigated limitations. A total of three comparisons made with the existing compliance/stiffness equations and FEA results indicated that the proposed empirical stiffness equations enlarge the range of rate of thickness to length and ensure the accuracy for each empirical stiffness equation under large deformation. The errors were within 6% when compared to FEA results.12 Dao and Huang focused on analysis and optimization for a rectangular leaf flexure hinge by employing pseudorigid-body model (PRBM) and the principle of virtual

work. Multi-objective structural optimization was carried out using the fuzzy logic based on Taguchi method. An input rotational angle was the most significant parameter with contribution of 44.2544%. The fatigue analysis determined that the mechanism could reach approximately 1million life cycles before failure.13 This article presents simple yet accurate approximations that capture the effects of load-stiffening and elastokinematic nonlinearities in beams. A general analytical framework is developed that enables a designer to parametrically predict the performance characteristics, such as mobility, over-constraint, stiffness variation, and error motions, of beam-based flexure mechanisms without resorting to tedious numerical or computational methods.14 This article deals with nonlinear analytical models of a class of compound multibeam parallelogram mechanisms (CBPMs) along with the static characteristic analysis. It is shown that the analytical primary motion model agrees with both the FEA model and the testing result very well, but the analytical parasitic motion model deviates from the FEA model over the large primary motion/force.15 In order to accurately model compliant mechanism utilizing plate flexures, this article investigates a quantitative equivalent modulus using nonlinear FEA to reflect coupled factors in affecting the modeling accuracy of two typical distributed compliance mechanisms. It has been shown that all parameters have influences on the equivalent modulus with different degrees, that the presence of large load-stiffening effect makes the equivalent modulus significantly deviate from the planar assumptions in two ideal scenarios, and that a plate modulus assumption is more reasonable for a very large out-of-plane thickness if the beam length is large.16 Extended nonlinear analytical modeling and analysis of compound parallelogram mechanisms are conducted in this article to consider the effect of the initial internal axial force. A physical preloading system to control the initial internal axial force is presented, and testing results of the object CBPM are compared with the theoretical ones.17 These researches have more attention on flexure hinge model building and its model error and prediction accuracy analysis. Some designs of flexure hinge have also been proposed and further optimized to obtain a structural optimization design. However, the positioning design of flexure hinge is interestingly investigated and usually ignored in performance of flexure hinge mechanism. This article will concentrate on the positioning design of flexure hinge and optimize the design by an optimization method combining ANSYS and MATLAB. The superior effectiveness of the optimal flexure hinge mechanism is validated by finite element numerical simulation and experiment.

s

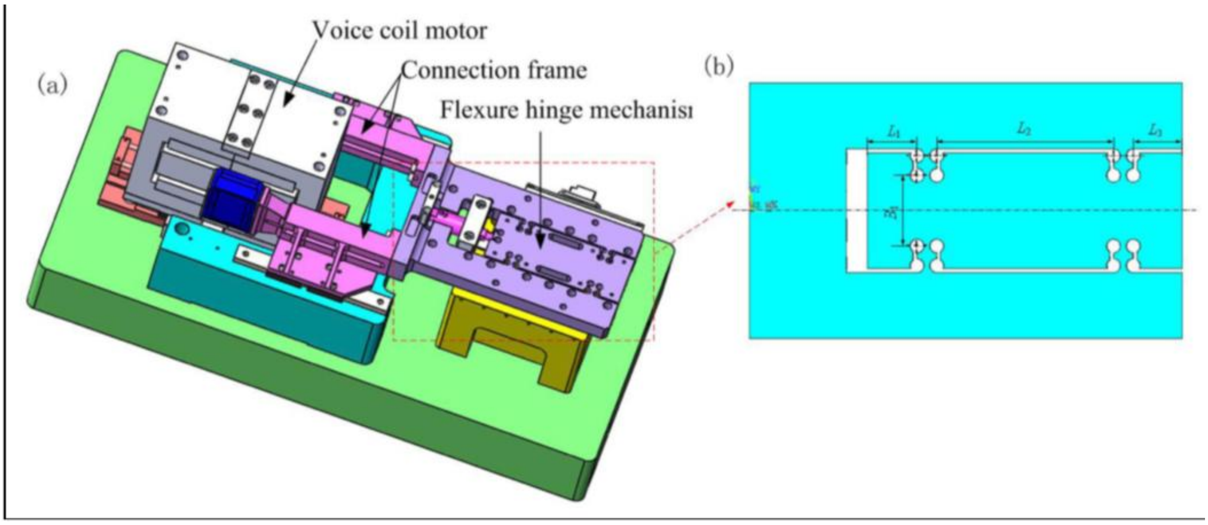

The Galaxy of K.S.R. Educational Institutions

K.S.Rangasamy college of Technology
K.S.R. Institute of Dental Science and Research
K.S.R.College of Engineering
K.S.R.Institute For Engineering and Technology
K.S.Rangasamy College of Arts & Science
K.S.Rangasamy College of Arts & Science for Women
K.S.Rangasamy Institute of Technology
K.S.R. Polytechnic College
K.S.R. College of Education
K.S.R. Matriculation Higher Secondary School
K.S.R. Industrial Training School
K.S.R. Akhsara Academy
Rajammal Rangasamy I.T.I.
Rajammal Rangasamy Teacher Training Institute
Rajammal Rangasamy Higher Secondary School
Avvai K.S.R. Matriculation School

SINCE 1984

K.S.R Instutitue for Engineering and Technology